hold a valid chemical fossil record[24].

Cyanobacterial BHP and 2-methyl-BHP may have oceanographic and palaeo-oceanographic applications as well, particularly with respect to evaluation of cyanobacterial primary productivity and their importance for the marine nitrogen and carbon cycles[25]. As biomarkers such as BHP and chlorophylls carry ^{13}C and ^{15}N signatures[16], their usefulness as tracers in modern aquatic and marine environments is significantly broadened. □

Methods

Total lipid extracts from cultures and environmental samples were analysed using a procedure modified and improved after ref. 8. Periodic acid oxidation followed by $NaBH_4$ reduction converted BHP to simpler hopanols amenable to purification by thin-layer chromatography and GC–MS analysis as acetate derivatives. BHP lacking a gem-diol function evade detection. The total number of culture samples with suitable data was 42 and, of these, only 6 failed to yield detectable hopanol. The data in Table 1 are from this study or directly extracted or calculated from published quantitative data.

The data for fossil hopanoids shown in Table 2 was derived from GC–MS–MS analyses[5] and based on the *m/z* 412 → 191 transition for αβ-hopane (3 in Fig. 1, R_3 = H) and *m/z* 426 → 205 for its 2α-methyl analogue (4, R_3 = H). These are expressed as the 2-methylhopane index = % 4/4+3. Accompanying C_{28}–C_{36} homohopanes (R = CH_3, R_3 = CH_3 to C_5H_7) were examined using the *m/z* 205 ion chromatograms and confirmed the relationships expressed here for the C_{30} and 2α-methyl C_{31} species. Age and lithology assignments for Phanerozoic samples were derived from AGSO databases. Assignments for Proterozoic sediments are primarily based on ref. 5, updated where possible. Numbers in parentheses indicate (*n*) samples of each rock unit. All samples are mature for oil generation except those marked with asterisks, which are above the oil window. Low 2α-methylhopane indices in these samples indicates incomplete release by thermal cracking of C_{35} and 2-Me C_{36} moieties bound in kerogen.

Received 23 March; accepted 11 June 1999.

1. Blankenship, R. E. & Hartman, H. The origin and evolution of oxygenic photosynthesis. *Trends Biochem. Sci.* **23,** 94–97 (1998).
2. Walter, M. R. in *Early Life on Earth* (ed. Bengtson, S.) 270–286 (Columbia Univ. Press, New York, 1994).
3. Schopf, J. W. Microfossils of the early Archean Apex Chert: New evidence of the antiquity of life. *Science* **260,** 640–646 (1993).
4. Buick, R. The antiquity of oxygenic photosynthesis: Evidence from stromatolites in sulfate-deficient Archaean lakes. *Science* **255,** 74–77 (1992).
5. Schopf, J. W. & Klein, C. *The Proterozoic Biosphere. A Multidisciplinary Study* (Cambridge Univ. Press, 1992).
6. Jürgens, U. J., Simonin, P. & Rohmer, M. Localisation and distribution of hopanoids in membrane systems of the cyanobacterium *Synechocystis* PCC 6714. *FEMS Microbiol. Lett.* **92,** 285–288 (1992).
7. Peters, K. E. & Moldowan, J. M. *The Biomarker Guide—Interpreting Molecular Fossils in Sediments and Petroleum* (Prentice-Hall, Englewood Cliffs, New Jersey, 1992).
8. Rohmer, M. The biosynthesis of triterpenoids of the hopane series in the eubacteria: a mine of new enzyme reactions. *Pure Appl. Chem.* **65,** 1293–1298 (1993).
9. Rohmer, M., Bouvier-Navé, P. & Ourisson, G. Distribution of hopanoid triterpenes in prokaryotes. *J. Gen. Microbiol.* **130,** 1137–1150 (1984).
10. Zundel, M. & Rohmer, M. Prokaryotic triterpenoids 3. The biosynthesis of 2β-methylhopanoids and 3β-methylhopanoids of *Methylobacterium organophilum* and *Acetobacter pasteurianus* spp. *pasteurianus*. *Eur. J. Biochem.* **150,** 35–39 (1985).
11. Simonin, P., Jürgens, U. J. & Rohmer, M. Bacterial triterpenoids of the hopane series from the prochlorophyte *Prochlorothrix hollandica* and their intracellular localisation. *Eur. J. Biochem.* **241,** 865–871 (1996).
12. Knani, M., Corpe, W. A. & Rohmer, M. Bacterial hopanoids from pink-pigmented facultative methylotrophs and from green plant surfaces. *Microbiology* **140,** 2755–2759 (1994).
13. Vilchèze, C., Llopiz, P., Neunlist, S., Poralla, K. & Rohmer, M. Prokaryotic triterpenoids: new hopanoids from the nitrogen-fixing bacteria *Azotobacter vinelandii*, *Beijerinckia indica* and *Beijerinckia mobilis*. *Microbiology* **140,** 2794–2753 (1994).
14. Renoux, J.-M. & Rohmer, M. Prokaryotic triterpenoids. New bacteriohopane tetrol cyclitol ethers from methylotrophic bacterium *Methylobacterium organophilum*. *Eur. J. Biochem.* **151,** 405–410 (1985).
15. Hermann, D. Des biohopanoïdes aux géohopanoïdes. Une approche de la formation des fossiles moléculaires de triterpénoïds en série hopane. Thesis, Univ. Haute-Alsace (1995).
16. Summons, R. E., Jahnke, L. L. & Simoneit, B. R. T. in *Evolution of Hydrothermal Ecosystems on Earth (and Mars?): Ciba Foundation Symposium 202* 174–194 (Wiley, Chichester, 1996).
17. Summons, R. E. & Jahnke, L. L. in *Biomarkers in Sediments and Petroleum* (eds Moldowan, J. M., Albrecht, P. & Philp, R. P.) 182–200 (Prentice Hall, Englewood Cliffs, New Jersey, 1992).
18. Summons, R. E. & Walter, M. R. Molecular fossils and microfossils of prokaryotes and protists from Proterozoic sediments. *Am. J. Sci. A* **290,** 212–244 (1990).
19. Bauld, J. in *Microbial Mats: Stromatolites* (eds Cohen, Y., Castenholz, R. W. & Halverson, H. O.) 39–58 (Alan Liss, New York, 1984).
20. Kenig, F. *et al.* Occurrence and origin of mono-, di-, and trimethylalkanes in modern and Holocene cyanobacterial mats from Abu Dhabi, United Arab Emirates. *Geochim. Cosmochim. Acta* **59,** 2999–3015 (1995).
21. Golubic, S. in *Early Life on Earth: Nobel Symposium No 84* (ed. Bengtson, S.) 220–236 (Columbia Univ. Press, New York, 1994).
22. Hayes, J. M., Summons, R. E., Strauss, H., Des Marais, D. J. & Lambert, I. B. in *The Proterozoic Biosphere: A Multidisciplinary Study* (eds Schopf, J. W. & Klein, C.) 81–133 (Cambridge Univ. Press, 1992.
23. Buick, R., Rasmussen, B. & Krapez, B. Archean oil: evidence for extensive hydrocarbon generation and migration 2.5–3.5 Ga. *AAPG Bull.* **82,** 50–69 (1998).
24. Price, L. C. Thermal stability of hydrocarbons in nature: limits, evidence, characteristics, and possible controls. *Geochim. Cosmochim. Acta* **57,** 3261–3280 (1993).
25. Haug, G. H. *et al.* Glacial/interglacial variations in production and nitrogen fixation in the Cariaco Basin during the last 580 kyr. *Paleooceanography* **13,** 427–432 (1998).
26. Bisseret, P., Zundel, M. & Rohmer, M. Prokaryotic triterpenoids: 2. 2β-methylhopanoids from *Methylobacterium organophilum* and *Nostoc muscorum*, a new series of prokaryotic triterpenoids. *Eur. J. Biochem.* **150,** 29–34 (1985).
27. Zhao, N. *et al.* Structures of two bacteriohopanoids with acyclic pentol side-chains from the cyanobacterium *Nostoc* PCC 6720. *Tetrahedron* **52,** 2772–2778 (1996).
28. Llopiz, P., Jürgens, U. J. & Rohmer, M. Prokaryotic triterpenoids: Bacteriohopanetetrol glycuronosides from the thermophilic cyanobacterium *Synechococcus* PCC6907. *FEMS Microbiol. Lett.* **140,** 199–202 (1996).

Acknowledgements. We thank D. Taylor for providing Hamersley basin samples and associated geological and maturity data. M. Rohmer, J. Hayes, K. Hinrichs, A. Knoll and M. Walter provided critical and constructive comments on drafts of this manuscript.

Correspondence and requests for material should be addressed to R.E.S. (e-mail: Roger.Summons@agso.gov.au).

Spatial scaling laws yield a synthetic theory of biodiversity

Mark E. Ritchie* & Han Olff†

* *Department of Fisheries and Wildlife, Utah State University, Logan, Utah 84322-5210, USA*

† *Tropical Nature Conservation and Vertebrate Ecology Group, Department of Environmental Science, Wageningen Agricultural University, Bornsesteeg 69, 6708 PD Wageningen, The Netherlands*

Ecologists still search for common principles that predict well-known responses of biological diversity to different factors[1–4]. Such factors include the number of available niches in space[5–7], productivity[8–10], area[10], species' body size[11–14] and habitat fragmentation. Here we show that all these patterns can arise from simple constraints on how organisms acquire resources in space. We use spatial scaling laws to describe how species of different sizes find food in patches of varying size and resource concentration. We then derive a mathematical rule for the minimum similarity in size of species that share these resources. This packing rule yields a theory of species diversity that predicts relations between diversity and productivity more effectively than previous models[8–10]. Size and diversity patterns for locally coexisting East African grazing mammals and North American savanna plants strongly support these predictions. The theory also predicts relations between diversity and area and between diversity and habitat fragmentation. Thus, spatial scaling laws provide potentially unifying first principles that may explain many important patterns of species diversity.

The search for a 'unified' theory of diversity[1–5] has focused on the premise that more species can exist within a habitat whenever they can more finely divide up space and different-sized resource 'packages'. Such partitioning may be constrained by the different body sizes of species[5,7,11,12–14], but the mechanisms by which organism size, resource availability and spatial structure of habitats control species diversity remain unclear[1,2,7,11,14]. Here we employ spatial scaling laws to describe how species with different body sizes find resources in space, and how limits to the similarity in body size between any two species predicts the potential number of species in a community.

Individual organisms must search within a space of suitable physical/chemical conditions (habitat) to find resources, which are often only available inside other material (food) (Fig. 1). Therefore, resources available to organisms are nested within food, and available food is nested within habitat. For example, insect herbivores move through suitable microclimates on terres-

trial plants (habitat) to eat plant tissue (food), which contains digestible carbohydrates (resources). Predatory fish search macrophyte-free areas of lakes (habitat) to eat invertebrates or smaller fish (food) that contain protein (resources). More imaginatively, terrestrial plants extend roots into rock-free soil (habitat) to take up soil solution (food) that contains nutrients (resources). Within a habitat, different species of similar trophic positions may harvest different sizes or types of food to obtain the same resources.

Distributions of habitat, food and resources often appear to be statistically self-similar (or self-affine) across ecologically relevant ranges of scales (3–4 orders of magnitude)[15,16]. If so, their volume or area and spatial distribution can be described with fractal geometry, that is, simple scaling laws. The total amount of habitat within a landscape of extent x is hx^D, where D is the fractal dimension of the habitat and h is a prefactor[17]. Likewise, food patches occupy a volume mx^F and resources occupy a volume rx^Q. The fractal dimensions D, F and Q represent the degree to which habitat, food and resources fill space, and can vary from 0 (a single point) to 3 (a filled cube). However, the assumption that habitat, food and resources are nested distributions[15] requires that $D \geq F \geq Q$. The prefactors h, m and r reflect the local density and contagion (lacunarity) of habitat, food and resources, respectively[15–17].

In a fractal environment, body size critically determines the abundance of food and resources that a species perceives[17–19] (Fig. 1). Individuals sample a volume of space at a particular scale of resolution: the length w of the 'ruler' with which they perceive or sample the environment. This scale of resolution is presumably proportional to body size. If so, a species will subdivide its habitat into subvolumes of size w^D. The volume w^D is the smallest food volume, or food-patch size P, consumed by the organism, that is, $w^D = P$. The total amount of food available to the organism is therefore the food contained in all subvolumes that it perceives as being filled with food, some of which are aggregated as larger food patches.

Larger species detect less total volume of food (only the larger patches) but can tolerate lower resource concentrations within their food, whereas smaller species detect more food (many small food patches), but require higher resource concentrations within it[14,17–19]. If individuals of a species search k sub-volumes of size P in a time period dt, and resources are instantaneously replaced following consumption, the population growth rate of the species can be described as $dN/dt = qN(kRBP - L)$ (ref. 20), where N is population size, q converts resources into individuals and L is resource loss rate. Food is encountered within the habitat at a density $B = mw^F/w^D$. Resources within food are encountered at a concentration $R = rw^Q/w^F$. As w is proportional to organism size, L will reflect the balance between greater metabolic rate and lower mortality for larger organisms, and be approximately size-invariant[21]. A species can persist if $kRBP \geq L$, which requires that

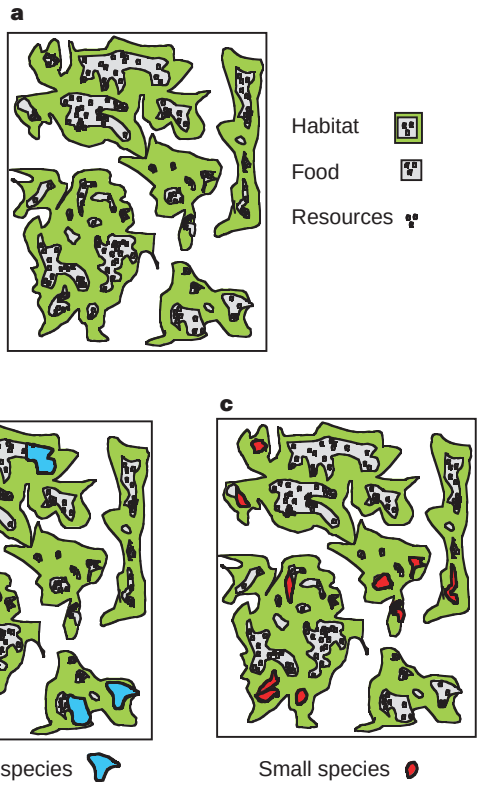

Figure 1 Hypothetical distribution of resources, food and habitat, as used by species of different size. **a**, Hypothetical space of extent x used by species of different size, including habitat, the food in which resources are contained and resources contained in food. Each element is fractal with the following mass fractal dimensions[17]: habitat: $D = 1.88$; food: $F = 1.53$; resource: $Q = 1.22$. Larger species (**b**) exclusively use large patches with low resource concentration, whereas smaller species (**c**) exclusively use small patches with high resource concentration. Note the 'microhabitat' separation in space of the two species' exclusive resources.

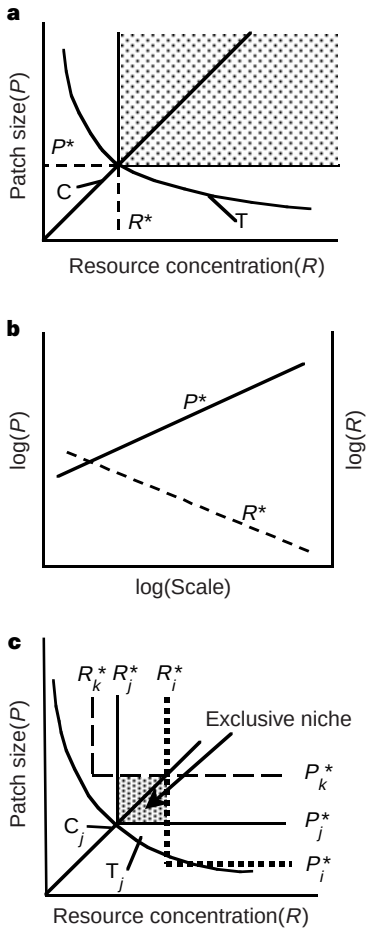

Figure 2 Graphical representation of the conditions for species persistence and coexistence. **a**, Minimum threshold patch size P^* and resource concentration R^* for a species. Increasing P implies that R can be reduced, yielding a trade-off relationship (curve T). However, larger patch sizes must be selected to encounter higher resource concentrations; that is, P is constrained to scale positively with R (line C). The intersection of curve T and line C yields the threshold P^*, R^* (equation (1)), which define suitable patches for the species (shaded area). **b**, Power law relationships for minimum food-patch size P^* and resource concentration R^* as a function of a species' size. **c**, Thresholds (R^*, P^*) for three species i, j, k that define the exclusive niche for species j (shaded area). Thresholds for species i and k will be positioned so that $P_j^* < P_k^*$ for every $R_j^* > R_i^*$ and to ensure that niche size $(P_k^* - P_j^*)(R_i^* - R_j^*)$ is large enough to ensure consumption rate ≥ loss rate.

a minimum food patch size (P^*) and minimum resource concentration (R^*) are exceeded. Greater P means that a lower R will meet resource losses, yielding a trade-off relationship: $P = Lw^{D-F}/(mkR)$ (curve T in Fig. 2a). However, larger organisms will encounter greater mean patch size but lower mean resource concentration in those patches. This encounter trade-off yields an 'encounter constraint' on the P and R that will satisfy resource losses. Substituting $R = rw^Q/w^F$ into the trade-off relationship yields the scaling law $P = Lw^{D-Q}/mkr$ and substituting $P = w^D$ yields $R = Lw^{-F}/mk$. Recognizing that the scaling law for R is imbedded in the scaling law for P yields the encounter constraint $P = R(1/r)w^{F+D-Q}$ (line C in Fig. 2a). Unique thresholds P^* and R^* emerge from the intersection of the trade-off relationship and encounter constraint. These are simply the square root of, for P^*, the product of patch size for replacing losses and expected patch size encountered, and, for R^*, the product of resource concentration for replacing resource losses and expected resource concentration.

$$P^* = (L/mkr)^{1/2}w^{D-Q/2}$$
$$R^* = (Lr/mk)^{1/2}w^{Q/2-F} \quad (1)$$

Because $D \geq F \geq Q$, P^* scales positively with size, whereas R^* scales negatively (Fig. 2b).

Applying these scaling laws to a group of species using similar resources, we find a 'packing' rule for how close in size species can be, that is, the size ratio γ between species of adjacent size. For a set of species i, j, k, ranked by increasing species size, the P^* and R^* of all three species define an exclusive niche for species j (Figs 1b, c, 2c): that is, both $P_i^* < P_j^* < P_k^*$ and $R_k^* < R_j^* < R_i^*$. For species j, there is a unique set of patches, ranging from size P_k^* to P_j^* and resource concentration R_i^* to R_j^*, that are both too small for species k and too low in resource concentration for species i. If the species is to persist regardless of the abundance of competitor species, the resource intake rate in time dt from these exclusive food patches must equal resource losses: $k(P_k^* - P_i^*)(R_i^* - R_j^*) = L$. We can now find γ by assuming that the size ratios for each of the two adjacent species pairs are equal ($\gamma = w_k/w_j = w_j/w_i$), and replacing w_k with γw_j and w_i with $(1/\gamma)w_j$ in equation (1) so that $P_k^* = (L/mkr)^{1/2}(\gamma w_j)^{D-Q/2}$ and $R_i^* = (Lr/mk)^{1/2}(w_j/\gamma)^{Q/2-F}$. The ratio γ will probably deviate from 1 by less than an order of magnitude, so $\gamma^{D-Q/2} \cong \gamma^{F-Q/2}$. With this assumption, we can substitute functions of γ for P_k^* and R_i^*, and, using equation (1) for P_j^* and R_j^*, we can approximately solve for γ as a function of species' size:

$$\gamma(w) \cong \{1 + m^{1/2}w^{(F-D)/2}\}^{1/(D-Q/2)} \quad (2)$$

The body-size ratio $\gamma(w)$ should therefore decline with increasing organism size (Fig. 3a). This is true because $D \geq F \geq Q$, and because small resource-rich patches needed by smaller species occupy proportionately less total volume than larger, resource-poor patches used by larger species. To test this size-ratio prediction, we analysed body size patterns for two guilds of species that use similar resources: co-occurring, East African grazing mammals that all eat primarily herbaceous plants[22–24] and vascular plants that compete for light in a Minnesota (USA) oak savanna[25]. Instead of being constant[1,5,11], size ratios in these very different assemblages declined significantly with increasing size (Fig. 3b, c), and the relationships fit the predicted shape (equation (2); Fig. 3a).

The functional equation for size ratios (equation (2)) dictates the number of species ranging in size from w_{min} to w_{max} that can be 'packed' into an environment. The maximum size (w_{max}) is determined by whether there is at least one suitable patch of size P^* and resource concentration R^* in a finite space of extent x. The number of suitable patches is found by dividing the total volume of resources rx^Q by the resource volume contained within suitable patches (P^*R^*). As P^* and R^* scale with w, however, the actual number of patches in the finite space is weighted by the probability of the occurrence of a patch with the length w specied by P^* and R^*. This probability is $(F-1)w^{-F}$ (ref. 19). Therefore, $(F-1)w^{-F}rx^Q/(P^*R^*) = 1$. Substituting for P^* and R^* (equation (1)) and solving for w yields

$$w_{max} = [(F-1)x^Qkrm/L]^{1/D} \quad (3)$$

A minimum resolution for a species within its environment (w_{min}) may ultimately be set by physical constraints to a particular body plan or prey size (for example, vertebrates, plankton and so on).

Species richness (S) is then the number of exclusive niches allowed between w_{min} and w_{max}, and is defined by

$$\prod_{i=1}^{S}\gamma(w_i) = \frac{w_{max}}{w_{min}} \quad (4)$$

which yields an approximate solution for S

$$S \cong \ln(w_{max})/[\gamma(w_{avg})\ln(w_{min})] \quad (5)$$

where w_{avg} is the mean body size in the guild. The functions implicit in w_{max} (equation (3)) and $\gamma(w_{avg})$ mean that the model also incorporates the effects on species richness of sampling area (x^2), habitat fragmentation (D) and the amount and distribution of food and resources (m, r, F, Q).

This model yields two unexpected predictions. First, it predicts a left-skewed, unimodal distribution of species richness versus organism size (Fig. 3d). This distribution reflects the larger size ratios and thus looser species packing required for smaller species (equation (2)) and the limitation of the largest species by the maximum patch size in the environment. The species richness–size distributions of both the East African herbivores and Minnesota plants are both significantly left-skewed (Fig. 3e, f), and differ from the log-normal or right-skewed distributions most commonly reported for species

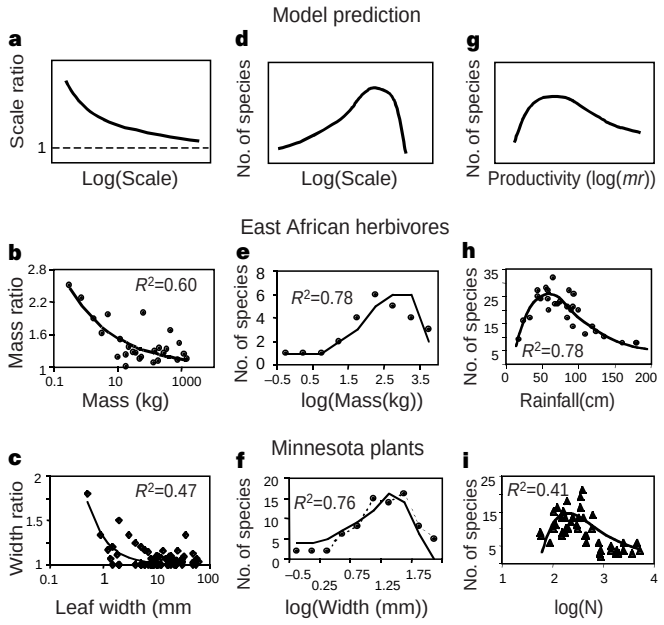

Figure 3 Predictions and tests of the scaling law model. **a**, Predicted size ratios (larger/smaller) for species of adjacent size versus size of the larger species; **d**, predicted number of species expected for communities versus log(size); and **g**, predicted number of species versus productivity, or log(mr). **b**, **c**, Observed size ratios (larger/smaller) of pairs of adjacent-sized species versus size of the larger of the pair. Size is body mass (kg) for Serengeti mammalian herbivores and leaf width (mm) for Minnesota plants. **e**, **f**, Observed frequency distributions of species richness versus classes of log(size) (dashed lines, closed circles). Both distributions are significantly left-skewed (D'Agostino test statistic, herbivores: –2.14; plants: –2.91, $P < 0.05$). **h**, Observed number of herbivore species versus annual precipitation for 28 different preserves in East Africa; and **i**, number of plant species per 0.9 m^2 across a gradient of available soil NH_4^+ plus NO_3^-. Solid lines (with R^2) in **b**, **c**, **e**, **f**, **h** and **i** are least-squares fits to nonlinear functions predicted by scaling laws.

grouped by taxa or biogeographic region[7,12,13]. Our model may not apply to communities that include species that use different resources or different habitats. Virtually all observed log-normal distributions combine diversity–size distributions of separate guilds (for example, nectarivores, granivores, herbivores, carnivores)[13] or species from different habitats[14].

Equation (5) also predicts the most commonly observed unimodal pattern of species richness versus productivity[8–10,26], namely that species richness should increase rapidly and then decline gradually in response to increased productivity (represented as $\log(mr)$, Fig. 3g). As resources become more abundant, maximum patch size rapidly increases to allow larger species to exist. However, further increases in resource abundance cause food patches to coalesce, eliminating small, resource-rich patches and requiring greater size separation among smaller species. Once again, the model's predictions are supported for the mammalian herbivore and plant communities we examined (Fig. 3h, i).

The application of spatial scaling laws indicates that many of the mechanisms controlling biodiversity may emerge from first principles of how organisms find resources in space. The analysis formalizes earlier ideas that diversity depends on the number of spatial niches[2,5,7,11], and indicates that coexisting species cannot infinitely partition space[9,10]. In addition, the model synthesizes recent ideas about how resource acquisition[12,14,27] and spatial characteristics of habitat[6,28] influence diversity. Clearly, other factors, including diversity of resource types[29], disturbance[4], colonization limitation[8,30] and biogeographical history[3,10,30], are also important in explaining diversity patterns. Nevertheless, the spatial scaling of resource use by species of different body size may explain many species-diversity patterns across a range of spatial scales and taxa. □

Methods

Size ratios (γ) and species richness (S) versus size relationships are for body mass of 27 mammalian grazer species >0.3 kg inhabitating open grasslands in the Serengeti National Park[22–24], and leaf width of 85 vascular plant species in a 1 ha of Minnesota oak savanna (leaves selected randomly on each of 10 plants of each species)[25]. The selected African savanna grazing mammals partition different parts of largely the same species of plants[22–24], and the Minnesota savanna plants potentially compete for light[25]. The number of >0.3 kg mammalian herbivore species found in 28 East African wildlife preserves was related to annual precipitation (a surrogate of productivity) at each preserve[23]. The August diversity of Minnesota plants was measured from biomass clipped in August 1989–1997 out of three 10 cm × 3 m strips within six replicate 81 m^2 plots that received either 0 or 26 g m^{-2} NH_4NO_3 per year since 1982 (ref. 25). Available $NH_4^+ + NO_3^-$ was measured with an Alpkem autoanalyser following 0.01 M KCl extractions of 2 × 15 cm deep soil cores[25]. The relationships between γ and the size of the larger of the species pair (to avoid negative autocorrelation), S and different size classes, and S and productivity (either rainfall or log(soil ammonium + nitrate)) were fitted to nonlinear functions predicted by the scaling model. The distributions of number of species versus log(size) were tested for skewness with D'Agostino tests.

Received 24 February; accepted 4 July 1999.

1. Brown, J. H. Two decades of homage to Santa Rosalia: toward a general theory of diversity. *Am. Zool.* **21,** 877–888 (1981).
2. May, R. M. How many species are there on earth? *Science* **241,** 1441–1449 (1988).
3. Schluter, D. & Ricklefs, R. (eds) *Species Diversity in Ecological Communities: Historical and Geographical Perspectives* (Univ. Chicago Press, Chicago, 1994).
4. Huston, M. A. *Biological Diversity: The Coexistence of Species on Changing Landscapes* (Cambridge Univ. Press, Cambridge, 1994).
5. Hutchinson, G. E. Homage to Santa Rosalia, or why are there so many kinds of animals? *Am. Nat.* **93,** 145–159 (1959).
6. MacArthur, R. H. Environmental factors affecting bird species diversity. *Am. Nat.* **98,** 387–397 (1964).
7. Morse, D., Stork, N. E. & Lawton, J. H. Fractal dimension of vegetation and the distribution of arthropod body lengths. *Nature* **314,** 731–732 (1985).
8. Tilman, D. & Pacala, S. W. in *Species Diversity in Ecological Communities: Historical and Geographical Perspectives* (eds Schluter, D. & Ricklefs, R.) 13–25 (Univ. Chicago Press, Chicago, 1994).
9. Rosenzeig, M. L. & Abramsky, Z. in *Species Diversity in Ecological Communities: Historical and Geographical Perspectives* (eds Schluter, D. & Ricklefs, R.) 52–65 (Univ. Chicago Press, Chicago, 1994).
10. Rosenzweig, M. L. *Species Diversity in Space and Time* (Cambridge Univ. Press, Cambridge, 1995).
11. Hutchinson, G. E. & MacArthur, R. H. A theoretical model of size distributions among species of animals. *Am. Nat.* **93,** 117–125 (1959).
12. Brown, J. H., Marquet, P. & Taper, M. Evolution of body size: consequences of an energetic definition of fitness. *Am. Nat.* **142,** 573–584 (1993).
13. Siemann, E., Tilman, D. & Haarstad, J. Insect species diversity, abundance and body size relationships. *Nature* **380,** 704–706 (1996).
14. Belovsky, G. E. Optimal foraging and community structure: the allometry of herbivore food selection and competition. *Evol. Ecol.* **11,** 641–672 (1997).
15. Milne, B. T. Spatial aggregation and neutral models in fractal landscapes. *Am. Nat.* **139,** 32–57 (1992).
16. Milne, B. T. in *Wildlife and Landscape Ecology: Effects of Pattern and Scale* (ed. Bissonette, J.) 32–69 (Springer, New York, 1997).
17. Mandelbrot, B. B. *The Fractal Geometry of Nature.* (Freeman, New York, 1983).
18. O'Neill, R. V., Milne, B. T., Turner, M. G. & Gardner, R. H. Resource utilization scales and landscape pattern. *Land. Ecol.* **2,** 63–69 (1988).
19. Ritchie, M. E. Scale-dependent foraging and patch choice in fractal environments. *Evol. Ecol.* **12,** 309–330 (1998).
20. Schoener, T. W. Population growth regulated by intraspecific competition for energy or time: some simple representations. *Theor. Pop. Biol.* **6,** 265–307 (1973).
21. Damuth, J. Population density and body size in mammals. *Nature* **290,** 699–700 (1981).
22. Sinclair, A. R. E. & Norton-Griffiths, M. (eds) *Serengeti: Dynamics of an Ecosystem* (Univ. Chicago, Chicago, 1979).
23. Kingdon, J. *East African Mammals: an Atlas of Evolution in Africa* Vol. 1–7 (Academic, New York, 1979).
24. Prins, H. H. T. & Olff, H. in *Dynamics of Tropical Communities* (eds Newbery, D. M., Prins, H. H. T. & Brown, N. D.) 449–490 (Blackwell, Oxford, 1998).
25. Ritchie, M. E., Tilman, D. & Knops, J. M. H. Effects of herbivores on plant and nitrogen dynamics in oak savanna. *Ecology* **79,** 165–177 (1998).
26. Grime, J. P. *Plant Strategies and Vegetation Processes* (Wiley, Chichester, 1979).
27. Wright, D. H. Species-energy theory: an extension of species-area theory. *Oikos* **41,** 496–506 (1983).
28. Palmer, M. W. The coexistence of species in fractal landscapes. *Am. Nat.* **139,** 375–397 (1992).
29. Jones, C. G. & Lawton, J. H. Plant chemistry and insect species richness of British umbellifers. *J. Anim. Ecol.* **60,** 767–777 (1991).
30. Hubbell, S. P. A unified theory of biogeography and relative species abundance and its application to tropical rainforests and coral reefs. *Coral Reefs* **16,** S9–S21 (1997).

Acknowledgements. We thank B. Milne, J. H. Brown, H. DeKroon, J. H. Emlen, S. Gripne, A. Guss, N. Haddad, L. Li, S. Naeem and W. Pitt for comments. Supported by the US NSF, The Netherlands NWO, Santa Fe Institute and USU Ecology Center.

Correspondence and requests for information should be addressed to M.R. (e-mail: ritchie@cc.usu.edu).

A mesoscale approach to extinction risk in fragmented habitats

Renato Casagrandi & Marino Gatto

Dipartimento di Elettronica e Informazione, Politecnico di Milano, Via Ponzio, 34/5, 20133 Milano, Italy

Assessing the fate of species endangered by habitat fragmentation[1–3] using spatially explicit and individual-based models[4–7] can be cumbersome and requires detailed ecological information that is often unavailable. Conversely, Levins-like[8] macroscale models[9,10] neglect data on the distribution of local numbers, which are frequently collected by field ecologists[11–13]. Here we present an alternative, mesoscale approach for metapopulations that are subject to demographic stochasticity, environmental catastrophes and habitat loss. Starting from a model that accounts for discrete individuals in each patch and assumes a birth–death stochastic process with global dispersal[14,15], we use a negative-binomial approximation[16] to derive equations for the probability of patch occupancy and the mean and variance of abundance in each occupied patch[17]. A simple bifurcation analysis[18] can be run to assess extinction risk. Comparison with both the original model and a spatially explicit model with local dispersal proves that our approximation is very satisfactory. We determine the sensitivity of metapopulation persistence to patch size, catastrophe frequency and habitat loss, and show that good dispersers are affected more by habitat destruction than by environmental disasters.

We consider an infinite network of equal patches with a uniform rain of propagules. We define $p_i(t)$ as the probability that, at time t, an integer number i of individuals is present in a patch; ν_i, μ_i and D_i as the birth, death and dispersal rates per capita in a patch containing i individuals; and m as the occurrence rate of catastrophes that wipe out a whole patch[19,20]. Because of dispersal mortality and/or inability to colonize, only a fraction a of the average number of